

Structural Properties and Phase Transitions of Y_2BaCuO_5 and $YBa_2Cu_3O_{9-\delta}$

H. Fjellvåg, P. Karen* and A. Kjekshus

Department of Chemistry, University of Oslo, Blindern, N-0315 Oslo 3, Norway

Fjellvåg, H., Karen, P. and Kjekshus, A., 1987. Structural Properties and Phase Transitions of Y_2BaCuO_5 and $YBa_2Cu_3O_{9-\delta}$. - Acta Chem. Scand., Ser. A 41: 283-293.

The properties of phases from the Cu-rich part of the Y-Ba-Cu-O phase diagram, with emphasis on the quaternary Y_2BaCuO_5 and $YBa_2Cu_3O_{9-\delta}$ phases, are considered. The green, semiconducting Y_2BaCuO_5 phase is confirmed to be a normal valence compound, and its structure is refined from powder neutron diffraction data. For the superconducting $YBa_2Cu_3O_{9-\delta}$ phase, four distinct modifications have been obtained on varying the conditions during the syntheses, and they differ in the manner of ordering of the oxygen atoms as well as in oxygen content. For the orthorhombic modifications a second-order transition to tetragonal variants takes place at 1100 ± 10 K, crystallographically implying a disordering of oxygen atoms.

The recent advances in the field of high-temperature superconductors represent a major breakthrough in one of the most challenging problems of material science, and open up for a probable technological revolution. The successful search for new high-temperature superconductors has revealed that such properties occur for a large family of structurally related quaternary oxides.¹⁻¹⁵ The current world record for high T_C may well be short-lived, since the race for optimum oxide systems is still in its very beginning.

In the Y-Ba-Cu-O system, the onset of superconductivity at temperatures around 93 K was first reported for samples of nominal composition $(Y_{1-x}Ba_x)_2CuO_{4-u}$ with $x \approx 0.4$ and u unspecified,⁴ which apparently were multi-phase samples consisting of black and green particles.^{5,13} Shortly before, high-temperature superconductivity ($T_C = 33$ K) was found for $La_{1.85}Ba_{0.15}CuO_4$,^{2,6} which is single-phase and adopts the K_2NiF_4 (also referred to as layered perovskite) type structure.⁶ The substitution of Ba into La_2CuO_4 causes a change from semiconducting to superconducting prop-

erties.⁶ However, none of the phases which occur in the Y-Ba-Cu-O system are of the K_2NiF_4 type. More recent studies of the Y-Ba-Cu-O system have demonstrated that the green constituent (of the above mentioned mixture) is the semiconducting compound Y_2BaCuO_5 ,^{8,14} The superconductivity is connected with the black $YBa_2Cu_3O_{9-\delta}$ ($\delta \approx 2$) phase.^{8,14,15} The crystal structure of the latter phase is an ordered variant of the structure of $La_{1.5}Ba_{1.5}Cu_3O_{9-\delta}$ (La and Ba randomly distributed over 2- and 4-fold positions). As expected, phases structurally related to $La_{1.85}Ba_{0.15}CuO_4$ and $YBa_2Cu_3O_{9-\delta}$ can be obtained when several other elements are exchanged for Y and/or Ba and still retain the superconductive properties.⁹⁻¹¹ A common structural feature of all these phases is the occurrence of planes (or arrays) of square-coordinated copper-to-oxygen networks going through the structure of an essentially perovskite-type atomic arrangement. The conductivity is, according to electronic band structure calculations, mainly due to $Cu(3d_{x^2-y^2}) - O(2p)$ interactions.¹⁸

The structural data, including here also composition and homogeneity range, for the superconducting phases are obviously burdened by the apparent demand for rapid publication in this

*On leave from Prague Institute of Chemical Technology, Department of Inorganic Chemistry, 166 28 Prague 6, Czechoslovakia.

field, and many reports lack crystallographic characterization of the samples studied. The four-component Y–Ba–Cu–O system contains an appreciable number of binary, ternary and quaternary phases whose crystal structures, thermal and physical properties were largely unknown before the rush for high-temperature superconductors started. In this study, some contributions to the Y–Ba–Cu–O phase diagram are provided, but the main emphasis is focused on the quaternary phases Y_2BaCuO_5 and $YBa_2Cu_3O_{9-\delta}$. Results obtained from powder X-ray and neutron diffraction, magnetic susceptibility and differential scanning calorimetry measurements are included. In particular, the connection between structural details and probable oxygen ordering schemes in $YBa_2Cu_3O_{9-\delta}$ is considered.

Experimental

Y_2O_3 (Megon, 99.999%), $BaCO_3$ (Merck, reagent grade) and CuO or Cu_2O (Merck, reagent grade) were used as starting materials. Mixtures in the desired proportions were finely ground and homogenized under acetone in a Fritsch Pulverisette laboratory grinder (three ~ 12 g agate balls) for 2 h. Pressed pellets of these samples were subsequently heated in corundum boats [platinum boats cannot be used because of their reaction with mixtures of $BaCO_3$ and RE_2O_3 ¹⁹ (RE = Rare earth element)] in air for 10–20 h at 900–1050°C. This process was generally repeated, up to 4–5 times. Both slow cooling ($100^\circ C h^{-1}$) down to 500°C, followed by cooling in air) and rapid quenching in air were adopted in the final annealing cycle. Various oxygen partial pressures during the synthesis or annealing of selected samples were obtained within the framework of the sealed silica-glass ampoule technique. Partial pressures of O_2 up to ~ 10 atm at 900°C were obtained by introducing controlled amounts of BaO_2 (Riedel de Haën AG, reagent grade). Very low partial pressures of O_2 during the annealing were provided by placing filings of Misch-metal in a separate corundum crucible placed together with the sample inside the sealed, evacuated ($\sim 10^2$ Pa) silica-glass tube. For the latter experiments prolonged reaction periods of up to 100 h were used. The use of closed silica-glass tubes also allowed rapid quenching of the samples in ice–water mixtures.

Chemical analysis of the Y–Ba–Cu–O samples was performed by classical, gravimetric methods. The samples were dissolved in 10 M hydrochloric acid. Barium was determined as $BaSO_4$, obtained by pouring the solution into a ten-fold volume of hot, 0.1 M H_2SO_4 solution when stirring, and drying the precipitate to constant weight at 600°C. Copper was determined in the filtrate as $CuSCN$.²⁰ Yttrium in the residual filtrate was precipitated by boiling with 6 M aqueous NH_3 solution. The $Y_2O_3 \cdot xH_2O$ product isolated by filtration was weighed as Y_2O_3 after burning of the paper filter and a 3 h heat treatment at 900°C.

Powder X-ray diffraction data were collected at room temperature with Guinier cameras ($CuK\alpha_1$ or $CrK\alpha_1$ radiation, Si as internal standard²¹). Position and intensity measurements of the reflections were carried out using a Nicolet L18 film scanner together with the SCANPI²² programme system. Trial and error indexing of the diffraction patterns was done with the TREOR²³ programme, and the GX²⁴ programme system was used in crystal structure refinements based on integrated intensities.

High-temperature powder X-ray diffraction data were collected with an Enraf-Nonius Guinier Simon camera ($CuK\alpha_1$ or $MoK\alpha_1$ radiation) between 20 and 1000°C. Unit cell dimensions were obtained by least-squares refinements using the CELLKANT²⁵ programme. Powder neutron diffraction data were collected with the OPUS III diffractometer located at a radial channel of the JEEP II reactor, Kjeller. Monochromated neutrons of wavelength 187.7 pm were used. The samples were placed in cylindrical vanadium sample holders, and data were collected in 2 θ steps of 0.05° between $2\theta = 5$ and 100° . Profile refinement was carried out according to the Rietveld²⁶ method, using the Hewat²⁷ version of the programme. The scattering lengths (in fm) $b_Y = 7.75$, $b_{Ba} = 5.25$, $b_{Cu} = 7.718$ and $b_O = 5.805$ were taken from Ref. 28.

Differential scanning calorimetry (DSC) measurements were made between 100 and 900 K with a Mettler TA 3000 thermo-analyzer system, using ~ 50 mg samples and sample holders of aluminium or evacuated, sealed silica-glass tubes. Data evaluation was done according to standard programmes for the system.

Magnetic susceptibility measurements were made using a Faraday balance (maximum field ~ 8 kOe) for temperatures between 80 and 1000 K.

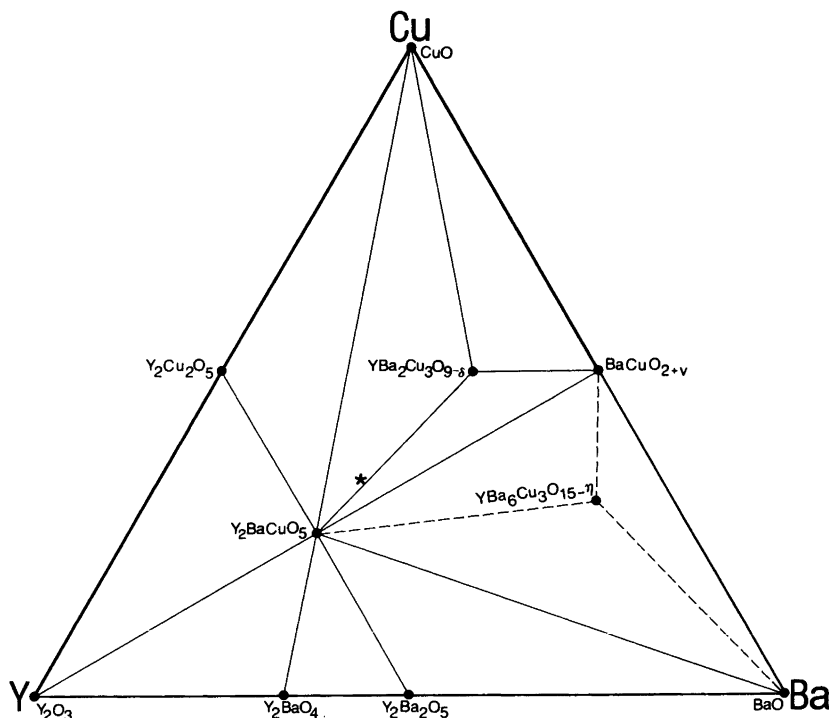


Fig. 1. Isothermal section of the Y-Ba-Cu-O phase diagram at $\sim 20^\circ\text{C}$ for samples prepared in air and slowly cooled from 900°C (the drawing represents a projection on an arbitrary plane with respect to oxygen content). The asterisk marks a nominal $Y_{1.20}Ba_{0.80}CuO_z$ mixture, filled circles distinct phases.

Results and discussion

(i) *Phase analysis.* Samples synthesized from mixtures of the oxides Y_2O_3 , $BaO(BaCO_3)$ and CuO in molar ratio 0.6 : 0.8 : 1.0, corresponding to the first reported⁴ superconducting materials of the Y-Ba-Cu-O system, proved to consist of several phases. An isothermal section through the Y_2O_3 -BaO-CuO phase diagram (projected on an arbitrary plane with respect to oxygen content) is shown in Fig. 1. The original mixture $Y_{1.2}Ba_{0.8}CuO_4$ is marked by an asterisk, whereas other ternary and quaternary phases can be identified by their chemical formulae. The present contribution to the phase diagram concerns mainly the Y_2O_3 -CuO-BaCuO₂ triangle, as indicated on the illustration.

The black appearance of our nominal $Y_{1.20}Ba_{0.80}CuO_z$ ($z \approx 3.65$) sample (when prepared at temperatures above 1000°C) is due to efficient coating of the green constituent by black

material, and a mechanical separation is hence not applicable. The nominal $Y_{1.20}Ba_{0.80}CuO_z$ mixture is completely soluble in a variety of acids (e.g. EDTA, CH_3COOH , HCl and HNO_3). A residue of $\sim 1\%$ (w/w) remaining after short term treatment with 0.1 M HNO_3 , was identified according to powder X-ray diffraction data as almost pure CuO , but with $\sim 1.5\%$ increased unit cell volume (obtained unit cell dimensions are $a = 468.5 \pm 0.1$, $b = 342.3 \pm 0.1$ and $c = 512.9 \pm 0.1$ pm, and $\beta = 99.54 \pm 0.02^\circ$; cf. the data for CuO in Ref. 29). X-Ray fluorescence measurements showed that the residue contains small amounts of Y which have probably replaced Cu by substitution, and this is the cause of the increased unit cell volume.

In aqueous NH_3 (preferably under CO_2 -free atmosphere, particularly when adding stoichiometric amounts of NH_4Cl with respect to the metal content of the sample) the black phase (and CuO) is brought into solution. The dissolution

process is greatly facilitated by continuous milling of the solid. In this way a green crystalline residue, amounting to $\sim 70\%$ (w/w) of the original bulk sample, is isolated. Chemical analysis gave a composition ratio Y : Ba : Cu $\approx 2.5 : 1 : 1$ for the green material, which is in accordance with the conclusion that this component is Y_2BaCuO_5 (which is indeed reported to be green³⁰) together with amorphous $\text{Y}_2\text{O}_3 \cdot x\text{H}_2\text{O}$ originating from the dissolution reaction when the black component is removed by the $\text{NH}_3/\text{NH}_4\text{Cl}$ treatment. The indexing of the powder diffraction pattern (all reflections accounted for) gave $a = 713.35 \pm 0.06$, $b = 1217.63 \pm 0.06$ and $c = 565.90 \pm 0.04$ pm for Y_2BaCuO_5 , in full conformity with results obtained previously by Michel and Raveau.³⁰ The virtually invariable unit cell dimensions of Y_2BaCuO_5 for samples with different nominal compositions (viz. independent of the nature and amounts of other phases present according to Fig. 1) show that this is a well-defined stoichiometric compound.

Subsequent analysis, of the black component (including minor amounts of CuO) has shown it to contain Y, Ba and Cu in the molar proportions $0.37 \pm 0.05 : 0.58 \pm 0.04 : 1.00 \pm 0.08$. Furthermore, the Bragg reflections from the black material, as for that found in multi-phase samples of nominal composition $\text{Y}_{1.2}\text{Ba}_{0.8}\text{CuO}_4$ after heat treatment above 1000°C , could be attributed to a tetragonal phase with $a = 385.66 \pm 0.06$ and $c = 1183.3 \pm 0.2$ pm. From volume increments estimated from data for the oxides, from the intensity distribution of the diffraction pattern and from chemical analyses, it was unambiguously concluded that the black material constitutes a tetragonal variant of $\text{YBa}_2\text{Cu}_3\text{O}_{9-\delta}$ [Refs. 8, 14, 15; see also (iii)]. Various other closely related tetragonal and orthorhombic variants of $\text{YBa}_2\text{Cu}_3\text{O}_{9-\delta}$ were obtained by re-annealing and by different cooling procedures. The unit cell volume for the tetragonal phase just mentioned is significantly larger than that for the orthorhombic variants ($176.00 \cdot 10^6$ versus $173.65 \cdot 10^6$ pm³), and this demonstrates a homogeneity range for the $\text{YBa}_2\text{Cu}_3\text{O}_{9-\delta}$ phase. Different aspects of the orthorhombic and tetragonal phases of $\text{YBa}_2\text{Cu}_3\text{O}_{9-\delta}$ are returned to in section (iii), but here it should be noted that independent of the route to $\text{YBa}_2\text{Cu}_3\text{O}_{9-\delta}$ in Fig. 1, the structurally distinct types of material produced are determined solely by the annealing conditions.

Concerning the phase diagram in Fig. 1, it should be noted that the Y_2BaCuO_5 phase is involved in equilibria with at least eight binary, ternary or quaternary phases, and thereby corresponds to a deep minimum in the Gibbs free energy surface associated with the diagram. The character of the phase diagram changes dramatically on turning to very low oxygen partial pressures, as e.g. obtained at 900°C under Mischmetal-gettered atmosphere in sealed silica-glass ampoules. Under the latter conditions the quaternary phases Y_2BaCuO_5 and $\text{YBa}_2\text{Cu}_3\text{O}_{9-\delta}$ decompose to Cu and ternary Y–Ba oxides. Under less extreme conditions it should be possible to retain e.g. the Cu(I) compounds BaCu_2O_2 ³¹ and YCuO_2 .³² On the other hand, phases containing Cu(III) are, when prepared in air, only obtained in the Ba-rich region of the phase diagram. Along the CuO– Y_2O_3 line one has to employ high oxygen partial pressures during the syntheses in order to obtain phases containing Cu(III).³³

The phase diagram (Fig. 1) exhibits a low-melting eutectic ($850\text{--}900^\circ\text{C}$) situated close to the $\text{YBa}_2\text{Cu}_3\text{O}_{9-\delta}$ -rich corner of the triangle with CuO and BaCuO_2 ($\text{BaCuO}_{2+\nu}$) as the other corners. During solidification of samples from this region, square-prismatically shaped single crystals of CuO are obtained *inter alia*. When solidified under an appropriate composition gradient, flexible platelets of $\text{YBa}_2\text{Cu}_3\text{O}_{9-\delta}$ of length up to $100\ \mu\text{m}$ and thickness $< 1\ \mu\text{m}$ are formed at the solid-liquid interface.

The present study provides also additional information on the ternary phases of the Y–Ba–Cu–O phase diagram. Most interesting is the existence of a hitherto unknown quaternary phase with a homogeneity range and composition close to that of $\text{Ba}_6\text{Cu}_3\text{O}_{15-\eta}$. The Y-rich end of this phase is tetragonal, $a = 580.5 \pm 0.1$ and $c = 802.3 \pm 0.2$ pm, and judged from the intensities of the Bragg reflections in the powder X-ray diffraction diagrams the structure is closely related to the perovskite type, with Y and Cu distributed over the octahedral sites in an ordered manner.

$\text{Y}_2\text{Cu}_2\text{O}_5$ is orthorhombic, $a = 1246.0 \pm 0.2$, $b = 1079.9 \pm 0.2$ and $c = 349.6 \pm 0.1$ pm. The $\text{RE}_2\text{Cu}_2\text{O}_5$ phases^{33–36} are structurally closely related to the $\text{In}_2\text{Cu}_2\text{O}_5$ type.³⁷ However, there are significant differences in the coordination around Cu^{2+} , mainly because of the disparity in size between In^{3+} and RE^{3+} .³⁵ The unit cell dimensions found for $\text{Y}_2\text{Cu}_2\text{O}_5$ match almost completely

those of $Ho_2Cu_2O_5$,³⁵ and are considerably larger than those of e.g. the Sc and Lu analogues³⁶ (some of the structural data for $Sc_2Cu_2O_5$ and $Y_2Cu_2O_5$ in Ref. 33 are likely to be incorrect). $Y_2Cu_2O_5$ is presently being further structurally characterized by means of powder neutron diffraction.

The $BaCuO_{2+\nu}$ ³⁸⁻⁴⁰ phase, as obtained in two-phase mixtures with $YBa_2Cu_3O_{9-\delta}$ after heat treatment at 900 °C, is cubic with $a = 1829.3 \pm 0.7$ pm. The non-stoichiometry parameter ν is evaluated to be ~ 0.05 from the relation between a and ν in Ref. 39. Well-developed, needle-shaped crystals of $BaCuO_{2+\nu}$ are formed on cooling a melt from 1000 °C. The colour of these changed lengthwise from transparent yellow (brown) to non-transparent black, which probably is a manifestation of continuous changes in ν (and consequently in the Cu(II)/Cu(III) atomic ratio) throughout the crystals.

(ii) *Structural properties of Y_2BaCuO_5 .* The green, orthorhombic Y_2BaCuO_5 phase adopts a well-known structure type found in a number of compounds.^{30,41} The copper atoms are coordinated by five oxygens forming an octahedron with one corner vacant, and these units are isolated from other CuO_5 units. The yttrium-oxygen coordination polyhedra are monocapped trigonal prisms, conjugated into Y_2O_{11} units, while the barium atoms have eleven oxygen neighbours in a more complex geometrical arrangement.^{30,41} As a means of comparing the structural characteristics of the semiconducting (normal valence compound) Y_2BaCuO_5 and superconducting

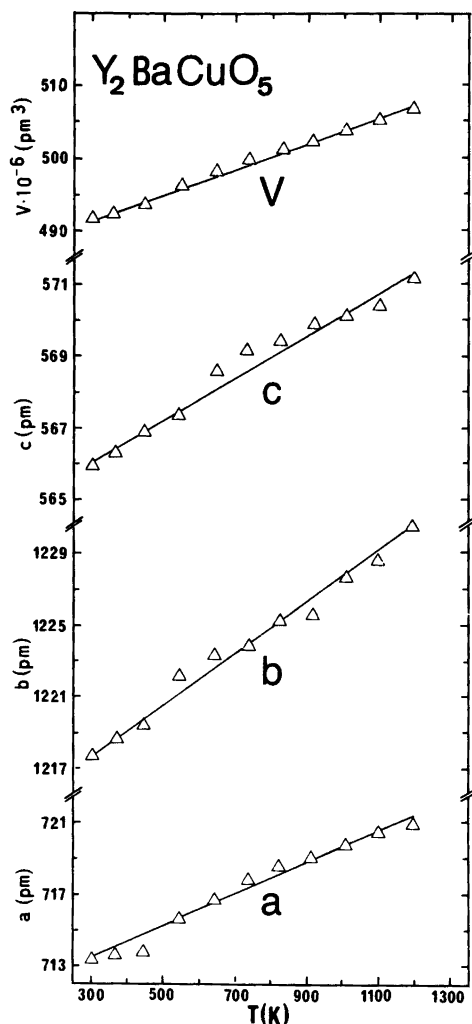


Fig. 2. Variation in unit cell dimensions of Y_2BaCuO_5 between 300 and 1200 K.

Table 1. Positional parameters for Y_2BaCuO_5 derived by Rietveld refinements of powder neutron diffraction data (space group $Pbnm$; Ba, Y and Cu in $4c$, O in $4c$ and $8d$; 130 reflections used in refinements; $R_n = 9.75$; calculated standard deviations in parentheses).

Atom	x	y	z
Ba	0.9266(22)	0.9089(16)	1/4
Y	0.3951(15)	0.0740(10)	1/4
Y	0.1264(19)	0.2881(8)	1/4
Cu	0.7147(15)	0.6602(11)	1/4
O	0.1680(9)	0.4324(8)	-0.0064(21)
O	0.3514(15)	0.2301(7)	0.5057(26)
O	0.9768(20)	0.0983(14)	1/4

$YBa_2Cu_3O_{9-\delta}$ phases, the coordination and the interatomic distances of the various atoms can be expressed in valence units of the central (metal) atoms by use of the bond-order concept.^{42,43} To our surprise, such analyses yield for the valence states of copper and yttrium in Y_2BaCuO_5 rather improbable values. The Zachariasen⁴³ approach gives 1.47 for the valence of copper (1.49 by the method of Brown and Shannon⁴²), and 2.73 and 3.64 valence units for the two crystallographically different yttrium atoms. These deviations from expected values initiated a re-examination of the

Y₂BaCuO₅ structure by powder neutron diffraction, in particular to refine the positional parameters of the oxygen atoms. The positional parameters thus derived are listed in Table 1; on the basis of these, quite reasonable values for the valence states (2.02 for copper, and 2.87 and 2.93 for yttrium) are now calculated.

High temperature Guinier Simon photographs of powder samples of Y₂BaCuO₅ revealed the absence of any structural phase transitions up to 1200 K (Fig. 2). The thermal expansion can be approximated to be linear over this temperature interval, with linear thermal expansion coefficients of $\alpha_a = (1/a_{300}) \cdot (\Delta a/\Delta T) = 1.2 \cdot 10^{-5}$, $\alpha_b = 1.2 \cdot 10^{-5}$, $\alpha_c = 1.0 \cdot 10^{-5}$ and $\alpha_v = 3.5 \cdot 10^{-5} \text{ K}^{-1}$.

In order to obtain supplementary, indirect structural information for Y₂BaCuO₅, DSC and magnetic susceptibility measurements between 80 and 900 K were carried out. DSC measurements, using evacuated, sealed silica-glass or open aluminium sample holders did not reveal any anomalies. The magnetic susceptibility of Y₂BaCuO₅ obeys the Curie-Weiss law over the temperature interval 80–1000 K, in accordance with Ref. 30. The effective paramagnetic moment, $\mu_{\text{eff}} = 2.15 \pm 0.20 \mu_B$ ($\theta = -50 \pm 20 \text{ K}$), is somewhat larger than expected for a “spin-only” 3d⁹ state (viz. 1.73 μ_B) and is indicative of some spin-orbit coupling.

(iii) *Structural properties of YBa₂Cu₃O_{9-δ}*. The structure of YBa₂Cu₃O_{9-δ} represents an ordered variant of the perovskite type where the ordering of Y and Ba, as well as of oxygen vacancies, causes tripling of the unit cell along the (tetragonal) *c* axis. The structure of an orthorhombic, at low temperatures superconducting, variant has recently been studied by means of powder neutron diffraction.¹⁵ The claims for both orthorhombic and tetragonal symmetry (see e.g. Refs. 8, 11, 14 and 15) indicate that YBa₂Cu₃O_{9-δ} exists in structurally different modifications. In this context it should be recalled that YBa₂Cu₃O_{9-δ} shows variable oxygen content and that the amount of oxygen influences the superconducting properties at low temperatures.^{8,14,16,17,44} Evidently, slight differences in conditions during the syntheses (maximum temperature, oxygen partial pressure and rate of cooling) govern a specific modification (viz. the degree and nature of vacancy ordering as well as site occupancy). The axial ratios *c/a* and *c/b* serve as indicators for the

structural relationship to the simple perovskite-type unit cell. In the following discussion of the orthorhombically distorted variants, the distortion parameter $\epsilon = |1 - a/b|$ is introduced.

In the present study, four different modifications of YBa₂Cu₃O_{9-δ} were identified without varying the preparation conditions dramatically. Line broadening of some reflections was frequently observed, which may indicate that within the concept of the distinct, basic types, intermediates of partially converted materials exist. However, the general resemblance of the diffraction patterns shows that all types adopt the same overall atomic arrangement. For the structurally related La_{1.5}Ba_{1.5}Cu₃O_{9-δ} phase,^{16,17} the composition parameter δ varies between 1.975 and 1.785, depending on the oxygen partial pressure during the heat treatment. It thus seems acceptable to advance the idea that variations in the number of vacancies and the ordering of these in the oxygen sub-lattice cause the existence of closely related phases of YBa₂Cu₃O_{9-δ}.

The four modifications can be classified according to their symmetry, axial ratios and distortion parameter:

type A: tetragonal with *c/a* ≈ 3

type B: tetragonal with *c/a* > 3

type C: orthorhombic with $2c/(a + b) \approx 3$
(*c/b* < 3) and $\epsilon \approx 0.007$

type D: orthorhombic with $2c/(a + b) > 3$
(*c/b* ≈ 3) and $\epsilon \approx 0.017$

Table 2. Unit cell dimensions of types A–D YBa₂Cu₃O_{9-δ} derived from powder X-ray diffraction studies. Calculated standard deviations in parentheses.

Type	<i>a</i> /pm	<i>b</i> /pm	<i>c</i> /pm	<i>V</i> ·10 ⁻⁶ /pm ³
A	387.22(9)		1161.5(2)	174.16(9)
B ^a	386.0(1)		1180.2(5)	175.89(14)
B	385.66(6)		1183.3(2)	176.00(7)
B ^b	390.1(1)		1192.0(5)	181.40(13)
C	385.2(1)	388.1(2)	1160.2(3)	173.44(11)
D	382.6(1)	388.8(1)	1167.7(2)	173.70(11)

^aRefers to bulk samples of nominal composition Y_{1.20}Ba_{0.80}CuO_{3.65}. ^bConverted from originally type D material, measured at 1040 K.

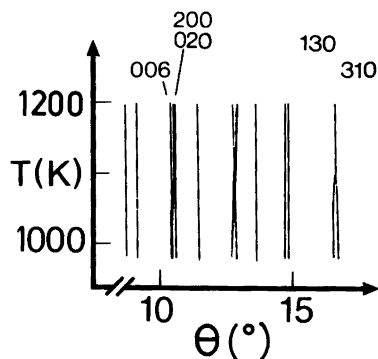


Fig. 3. Selected part, drawn schematically, of a high-temperature Guinier Simon photograph for $\text{YBa}_2\text{Cu}_3\text{O}_{9-\delta}$, type D.

Refined unit cell dimensions for the types A-D $\text{YBa}_2\text{Cu}_3\text{O}_{9-\delta}$ are given in Table 2.

The type B structure is reported in the literature for a number of phases with general composition $\text{REBa}_2\text{Cu}_3\text{O}_{9-\delta}$ ($\text{RE} = \text{Nd}, \text{Sm}, \text{Eu}$ or Gd) in addition to $\text{YBa}_2\text{Cu}_3\text{O}_{9-\delta}$.^{10,11} This variant is found in the bulk, two-phase samples of nominal composition $\text{Y}_{1.2}\text{Ba}_{0.8}\text{CuO}_2$ heat-treated above $\sim 1000^\circ\text{C}$. It is readily obtained from melts, the manner of cooling being then less significant. The type A variant is found for samples synthesized under oxygen pressures of ~ 10 atm (using peroxide, see Experimental) and quenched from high temperatures (say, above 900°C ; an axial ratio $c/a \approx 3$ is also found for the $\text{La}_{1.5}\text{Ba}_{1.5}\text{Cu}_3\text{O}_{9-\delta}$ -related phases).^{16,17} The type C structure is established for samples synthesized under oxygen pressures of ~ 10 atm (using peroxide) and slowly cooled from 900°C . The fourth type, D, is obtained for samples heat-treated at temperatures below the melting points and allowed to cool slowly. When considering the recently published data on $\text{REBa}_2\text{Cu}_3\text{O}_{9-\delta}$,¹⁰ it is realized that these, in general, orthorhombic phases exhibit axial ratios $c/b > 3$ and $c/a > 3$, while $0.003 \leq \epsilon \leq 0.008$. It should be stressed that the classification scheme outlined above applies to $\text{YBa}_2\text{Cu}_3\text{O}_{9-\delta}$, and that chemical substitution may change the axial ratios and the degree of distortion.

The structural properties of type A-D $\text{YBa}_2\text{Cu}_3\text{O}_{9-\delta}$ samples between 300 and 1300 K, i.e. temperatures approaching those used during the preparation, were judged from Guinier Si-

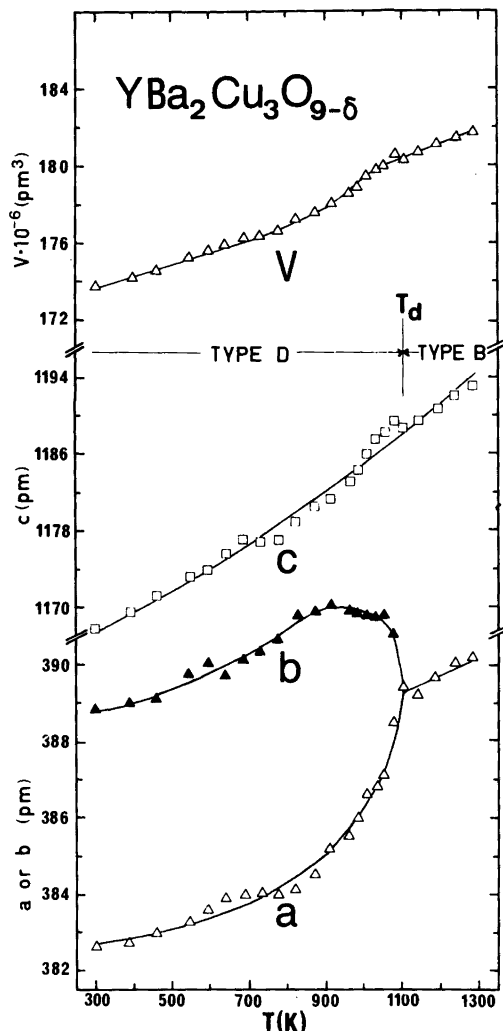


Fig. 4. Variation in unit cell dimensions of $\text{YBa}_2\text{Cu}_3\text{O}_{9-\delta}$, type D, between 300 and 1300 K.

mon photographs. Fig. 3 shows a schematic drawing of a selected part of the powder X-ray diffraction pattern of a type D phase (under sealed silica-glass capillary conditions) between 900 and 1200 K. At 900 K, the 006 and 020 reflections overlap and are well separated from the neighbouring 200 reflection. On heating to some 1000 K, 020 and 200 start to approach each other before finally merging into one single reflection for $T \geq T_d = 1100 \pm 10$ K. In open capillaries the transition is shifted some 150 K towards lower

temperature. The variation of the unit cell dimensions with temperature is shown in Fig. 4, and the reversible phase transition from orthorhombic to tetragonal (type B) structure progresses smoothly without discontinuous changes in unit cell dimensions, lacks detectable hysteresis and may hence be classified as second-order. The variation of the distortion parameter ϵ with the reduced temperature T/T_d is shown in Fig. 5. A continuous change in unit cell volume is observed around T_d . The thermal expansion is non-linear with temperature, however, the *average* thermal expansion coefficient calculated over the temperature range 300–1100 K for the type D phase being $\alpha_V = 4.8 \cdot 10^{-5} \text{ K}^{-1}$.

Similar high temperature studies were performed for the types A, B and C. For neither A nor B were there any indications of phase transitions between 300 and 1200 K, the thermal dependence of the unit cell dimensions of the type A variant being given as an illustrative example in Fig. 6. The linear thermal expansion coefficients (Fig. 6) for temperatures between 300 and 1200 K are $\alpha_a = 1.2 \cdot 10^{-5}$, $\alpha_c = 1.3 \cdot 10^{-5}$ and $\alpha_V = 3.6 \cdot 10^{-5} \text{ K}^{-1}$. For the orthorhombic type C, a phase transition resembling that observed for orthorhombic type D could be expected, and this was indeed observed at $T_d = 1100 \pm 10 \text{ K}$.

Several isotopic homologues of $\text{YBa}_2\text{Cu}_3\text{O}_{9-\delta}$ have recently been reported,^{9-11,13} in which yttrium is partially or completely replaced by a 4f element while retaining the high superconducting transition temperature. Similar homologues have also been reported for $\text{La}_{1.5}\text{Ba}_{1.5}\text{Cu}_3\text{O}_{9-\delta}$, with RE

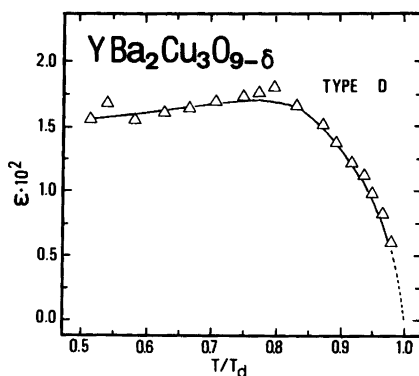


Fig. 5. Temperature dependence of the orthorhombic distortion parameter (ϵ) for the type D \rightleftharpoons B second-order phase transition of $\text{YBa}_2\text{Cu}_3\text{O}_{9-\delta}$.

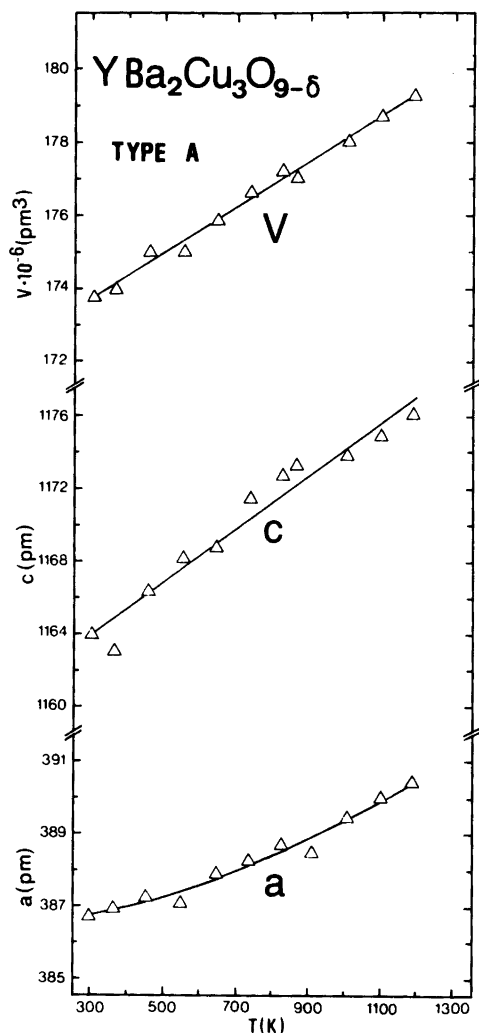


Fig. 6. Variation in unit cell dimensions of $\text{YBa}_2\text{Cu}_3\text{O}_{9-\delta}$, type A, between 300 and 1200 K.

replacing La.¹⁷ Their physical properties have until now not been examined. The fact that for the latter phases $cla \approx 3$ (actually $\sqrt{2} \cdot cla_p$; see below), as opposed to $cla > 3$ (even with orthorhombic distortion) for the former phases, may indicate either disorder of RE and Ba in the $\text{La}_{1.5}\text{Ba}_{1.5}\text{Cu}_3\text{O}_{9-\delta}$ analogues, or the existence of a solid solution region where RE partially replaces Ba, or an appreciably different ordering scheme for oxygen atoms in the two series of phases.

A common structural building element of all

the new high-temperature superconducting phases (perovskite-related or K_2NiF_4 type) is an infinite network of interconnected square-planar CuO_4 groups. The short Cu–O bonds and the regularity of this sub-lattice arrangement appear to be key structural ingredients for the occurrence of high-temperature superconductivity. A major distinction between the quaternary copper oxides of the perovskite-related type and the K_2NiF_4 type⁶ is the large number of oxygen vacancies for $YBa_2Cu_3O_{9-\delta}$ and its isotypic homologues. These vacancies have to appear since lower-valent cations (in this case Ba^{2+}) are introduced in the (basic perovskite type) lattice without being conventionally charge-compensated by other cations.

In the structure of $YBa_2Cu_3O_{9-\delta}$, six different sites for oxygen are possible (derived from the basic perovskite-type structure; orthorhombic, space group $Pmmm$): O(1) in $2q$ ($0,0,z$; $z \approx 0.17$), O(2) in $2s$ ($\frac{1}{2},0,z$; $z \approx 0.33$), O(3) in $2r$ ($0,\frac{1}{2},z$; $z \approx 0.33$), O(4) in $1e$ ($0,\frac{1}{2},0$), O(5) in $1b$ ($\frac{1}{2},0,0$) and O(6) in $1c$ ($0,0,\frac{1}{2}$). Experimental values for the lower limit of δ are around two, and different ordering schemes for the oxygen atoms over the possible sites have been put forward. Siegrist *et al.*⁴⁵ suggested for $YBa_2Cu_3O_{9-\delta}$ that the $1c$ site is empty, one oxygen is disordered over the $1b$ and $1e$ sites, and the other positions are completely filled. Capponi *et al.*¹⁵ report similar findings, except that the $1b$ site is empty and the $1e$ site filled. For $La_{1.5}Ba_{1.5}Cu_3O_{9-\delta}$ the results obtained by Er-Rakho *et al.*¹⁷ (for an enlarged cell $\sqrt{2}a_p, \sqrt{2}a_p, 3a_p$) establish that no oxygen vacancies occur within the two-dimensional CuO_4 networks.

Based on the neutron diffraction results of Capponi *et al.*,¹⁵ some considerations concerning the defect structure of the type A–D variants of $YBa_2Cu_3O_{9-\delta}$ can be put forward. The ordered oxygen vacancies within the Cu layer at $z = 0$ cause a contraction of the orthorhombic a axis ($\epsilon \approx 0.017$), indicating that the vacancy is smaller than the corresponding oxygen atom. Moreover, the present considerations on the relationship between the unit cell dimensions and defect structure assume that the metal atoms do not significantly change positions in the structure even if the ordering of the oxygen atoms is markedly different. Hence, it is believed that for the purpose of elucidating the above mentioned structural relations one can restrict oneself to consid-

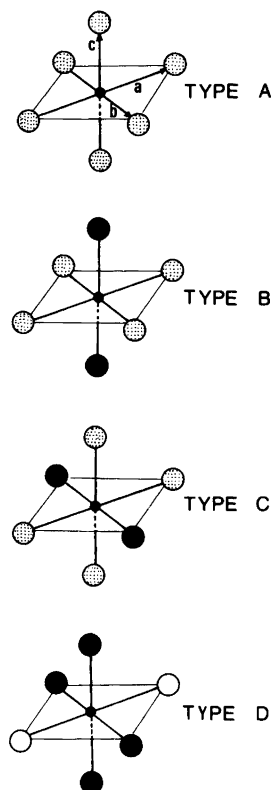


Fig. 7. Idealized defect structure of the CuO_6 octahedron for Cu in $z = 0$ for type A–D variants of $YBa_2Cu_3O_{9-\delta}$.

ering the defect structure of the CuO_6 octahedron for Cu in $z = 0$. The suggested ordering schemes for the type A–D variants are illustrated in Fig. 7, elaborated under the assumption of constant oxygen content for all types. Type D, which corresponds to the structure described by Capponi *et al.*,¹⁵ represents a completely ordered variant, while type A is completely disordered with four oxygens randomly distributed over six positions.

The very existence of different variants of $YBa_2Cu_3O_{9-\delta}$ and temperature-induced phase transitions are strong indications of the important role of the vacancy ordering. At elevated temperatures the higher oxidation state of copper becomes unstable, which will cause a change in composition towards higher δ . The increase in unit cell volume for type D samples around T_d may reflect such changes, or reflect different size requirements of ordered and disordered vacancies. However, it is tempting to suggest that

the driving force for, e.g., the second-order phase transition between the type D and type B phases is the free energy gain by disordering of oxygen atoms (and vacancies) at T_d . For $T \ll T_d$, vacancies and oxygen atoms should be ordered,¹⁵ while for $T > T_d$ these (probably in lower concentration) are randomly distributed over the CuO_4 unit within the basal plane at $z = 0$. The extraordinary dependence of the physical properties of $\text{YBa}_2\text{Cu}_3\text{O}_{9-\delta}$ on the oxygen partial pressure during the synthesis strongly suggests that the vacancy order as well as the vacancy concentration significantly influences the conductivity properties.

Magnetic susceptibility measurements on the superconducting⁴⁶ $\text{YBa}_2\text{Cu}_3\text{O}_{9-\delta}$ variants reveal weak, almost temperature-independent paramagnetism above $T_C \approx 93$ K (and, of course, diamagnetism below T_C), reflecting that the main contribution originates from conduction electrons and that no localized moments exist on the Cu atoms.

Acknowledgements. We would like to thank Dr. A. F. Andresen, Institute for Energy Technology, for skilful assistance in the powder neutron diffraction experiments. P. K. acknowledges the award of an exchange fellowship under the cultural agreement between Czechoslovakia and Norway.

References

1. Bednorz, J. G. and Müller, K. A. *Z. Phys. B* 64 (1986) 189.
2. Chu, C. L., Hor, P. H., Meng, R. L., Gao, L., Huang, Z. J. and Wang, Y. Q. *Phys. Rev. Lett.* 58 (1987) 405.
3. Cava, R. J., van Dover, R. B., Batlogg, B. and Rietman, E. A. *Phys. Rev. Lett.* 58 (1987) 408.
4. Wu, M. K., Ashburn, J. R., Torng, C. T., Hor, P. H., Meng, R. L., Gao, L., Huang, Z. J., Wang, Y. Q. and Chu, C. H. *Phys. Rev. Lett.* 58 (1987) 908.
5. Hor, P. H., Gao, L., Meng, R. L., Huang, Z. J., Wang, Y. Q., Forster, K., Vassiliou, J., Chu, C. W., Wu, M. K., Ashburn, J. R. and Torng, C. T. *Phys. Rev. Lett.* 58 (1987) 911.
6. Jørgensen, J. D., Schüttler, H. B., Hinks, D. G., Capone, D. W., Zhang, K., Brodsky, M. B. and Scalapino, D. J. *Phys. Rev. Lett.* 58 (1987) 1024.
7. Sun, J. Z., Webb, D. J., Naito, M., Char, K., Hahn, M. R., Hsu, J. W. P., Kent, A. D., Mitzi, D. B., Oh, B., Beasley, M. R., Geballe, T. H., Hammond, R. H. and Kapitulnik, A. *Phys. Rev. Lett.* 58 (1987) 1574.
8. Cava, R. J., Batlogg, B., van Dover, R. B., Murphy, D. W., Sunshine, S., Siegrist, T., Remeika, J. P., Rietman, E. A., Zahurak, S. and Epifosa, G. P. *Phys. Rev. Lett.* 58 (1987) 1676.
9. Moodenbaugh, A. R., Suenaga, M., Asano, T., Shelton, R. N., Ku, H. C., McCallum, R. W. and Klavins, P. *Phys. Rev. Lett.* 58 (1987) 1885.
10. Murphy, D. W., Sunshine, S., van Dover, R. B., Cava, R. J., Batlogg, B., Zahurak, S. M. and Schneemeyer, L. F. *Phys. Rev. Lett.* 58 (1987) 1888.
11. Hor, P. H., Meng, R. L., Wang, Y. Q., Gao, L., Huang, Z. J., Bechtold, J., Forster, K. and Chu, C. W. *Phys. Rev. Lett.* 58 (1987) 1891.
12. Wang, H. H., Geiser, U., Thorn, R. J., Carlson, K. D., Beno, M. A., Monaghan, M. R., Allen, T. J., Proksch, R. B., Stupka, D. L., Kwok, W. K., Crabtree, G. W. and Williams, J. M. *Inorg. Chem.* 26 (1987) 1190.
13. Stacy, A. M., Badding, J. V., Geselbracht, M. J., Ham, W. K., Holland, G. F., Hoskins, R. L., Keller, S. W., Millikan, C. F. and zur Loye, H. C. *J. Am. Chem. Soc.* 109 (1987) 2528.
14. Rao, C. N. R., Ganguly, P., Raychaudhuri, A. K., Mohan Ram, R. A. and Sreedhar, K. *Nature (London)* 326 (1987) 856.
15. Capponi, J. J., Chailout, C., Hewat, A., Lejoy, P., Marezib, M., Ngyen, N., Raveau, B., Soubeyroux, J. L., Tholence, J. L. and Tournier, R. *Europhys. Lett.* 3 (1987) 1301.
16. Michel, C., Provost, J., Studer, F. and Raveau, B. *Stud. Inorg. Chem.* 3 (1983) 357.
17. Er-Rakho, L., Michel, C., Provost, J. and Raveau, B. *J. Solid State Chem.* 37 (1981) 151.
18. Yu, J., Freeman, A. J. and Xu, J. H. *Phys. Rev. Lett.* 58 (1987) 1035.
19. Schiffler, S. and Müller-Buschbaum, H. *Z. Anorg. Allg. Chem.* 523 (1985) 63.
20. Kolthoff, I. M. and Sandell, E. B. *Textbook of Quantitative Inorganic Analysis*, MacMillan, New York - Chicago - Dallas - Atlanta - San Francisco - Toronto 1952.
21. Deslatters, R. D. and Henins, A. *Phys. Rev. Lett.* 31 (1973) 972.
22. Werner, P. E. *The Computer Programme SCANPI* [Scan Calculate Analyze Numerical Powder Intensities] Institute of Inorganic Chemistry, University of Stockholm, Stockholm, Sweden 1981.
23. Werner, P. E. *Z. Kristallogr.* 120 (1964) 375.
24. Mallinson, P. and Muir, K. W. *J. Appl. Crystallogr.* 18 (1984) 51.
25. Ersson, N. O. *Program CELLKANT*, Chemical Institute, Uppsala University, Uppsala, Sweden 1981.

26. Rietveld, H. M. *J. Appl. Crystallogr.* 1 (1968) 65.
27. Hewat, A. W. *The Rietveld Computer Program for the Profile Refinement of Neutron Diffraction Powder Patterns Modified for Anisotropic Thermal Vibrations*. UKAERE Harwell Rep. RRL 73/897, Harwell 1973.
28. Koester, L. and Yelon, W. B. In: Yelon, W. B., Ed., *Neutron Diffraction Newsletter*, The Neutron Diffraction Commission, Missouri 1983.
29. Pearson, W. B. *Handbook of Lattice Spacings and Structures of Metals and Alloys*, Pergamon, Oxford - London - Edinburgh - New York - Toronto - Paris - Braunschweig 1967.
30. Michel, C. and Raveau, B. *J. Solid State Chem.* 43 (1982) 73.
31. Teske, C. L. and Müller-Buschbaum, H. *Z. Naturforsch.* B 27 (1972) 296.
32. Köhler, B. U. and Jansen, M. *Z. Anorg. Allg. Chem.* 543 (1986) 73.
33. Arjomand, M. and Machin, D. J. *J. Chem. Soc., Dalton Trans.* (1975) 1961.
34. Schmitz-Dumont, O. and Kasper, H. *Monatsh. Chem.* 96 (1965) 506.
35. Freund, H. R. and Müller-Buschbaum, H. *Z. Naturforsch.* B 32 (1977) 609.
36. Freund, H. R. and Müller-Buschbaum, H. *Z. Naturforsch.* B 32 (1977) 1123.
37. Begerhoff, G. and Kasper, H. *Acta Crystallogr., Sect. B* 24 (1968) 388.
38. Kipka, R. and Müller-Buschbaum, H. *Z. Naturforsch.* B 32 (1977) 121.
39. Migeon, H. N., Zanne, M., Jeannot, F. and Gleitzer, C. *Rev. Chim. Miner.* 14 (1977) 498.
40. Migeon, H. N., Jeannot, F., Zanne, M. and Aubry, J. *Rev. Chim. Miner.* 13 (1976) 440.
41. Michel, C. and Raveau, B. *J. Solid State Chem.* 49 (1983) 150.
42. Brown, I. D. and Shannon, R. D. *Acta Crystallogr., Sect. A* 29 (1973) 266.
43. Zachariasen, W. H. *J. Less-Common Met.* 62 (1978) 1.
44. Engler, E. M., Lee, V. Y., Nazzari, A. I., Beyers, R. B., Lim, G., Grant, P. M., Parkin, S. S. P., Ramirez, M. L., Vazquez, J. E. and Savoy, R. J. *J. Am. Chem. Soc.* 109 (1987) 2848.
45. Siegrist, T., Sunshine, S., Murphy, D. W., Cava, R. J. and Zahurak, S. M., *APS Meeting*, New York, March 1987.
46. Fjellvåg, H., Karen, P., Kjekshus, A., Bratsberg, H., Helgesen, G. and Andresen, A. F. *To be published*.

Received July 2, 1987.